PHYSICAL REVIEW B **77**, 140401(R) (2008)

Effect of ferromagnetism on AB oscillations in a normal-metal ring

Koji Sekiguchi,* Akinobu Yamaguchi, and Hideki Miyajima
Department of Physics, Keio University, Hiyoshi 3-14-1, Yokohama 223-8522, Japan

Atsufumi Hirohata
Department of Electronics, University of York, Heslington, York YO10 5DD, United Kingdom
(Received 18 January 2008; revised manuscript received 4 March 2008; published 2 April 2008)

Quantum phase modulation is achieved in a metallic nanoring with a FeNi/Cu/FeNi (ferromagnet/normal-metal/ferromagnet) layer. Both frequency and amplitude of Aharonov-Bohm oscillation are found to be modified with respect to the magnetization configurations, indicating that the phase modulation originates from the spin-orbit scattering induced by the magnetization of the ferromagnets. Such phase modulation is "crossover" phenomena between mesoscopic magnetism and microscopic quantum interference effects, which provides fundamental knowledge upon quantum spin transport.

DOI: 10.1103/PhysRevB.77.140401 PACS number(s): 75.47.De, 72.15.Gd, 72.25.Ba, 72.25.Mk

Quantum phases of charged particles have intensively been investigated in mesoscopic structures, and have revealed interference and oscillatory behavior induced by an external field application. For instance, electrons traveling along semiconductor (and normal metal) rings threaded by a magnetic flux acquire a quantum dynamical phase, producing interference phenomenon such as Aharonov-Bohm (AB) and Altshuler-Aronov-Spivak (AAS) effects.[1–5] In addition, when a spin of electron rotates during its orbital motion along the ring-shaped path, the electron acquires an additional phase contribution known as the geometrical phase (Berry phase).[6–8]

Recently, prominent phenomenon in virtue of a geometrical phase has been predicted by studying electron transport under an inhomogeneous magnetic field; the geometrical phase can drive a persistent current.[9,10] Pioneering experiment has been performed with using a spin-orbit scattering in two-dimensional electron gas (2DEG) semiconductor, which also strongly couples spin and orbital motion and introduces the spin rotation.[11] For metallic rings, it has theoretically been pointed out that electrons can sense the geometrical phase even when an effective exchange field is induced by ferromagnets.[12] However, no results have been reported on the correlation between the geometrical phase and the presence of the ferromagnets to date. Interestingly, as oppose to general belief that ferromagnets destroy any quantum phase effects due to their complex dephasing mechanisms, an oscillatory behavior of resistance in a permalloy nanoring has been observed,[13] and an effect of ferromagnetic ordering in a GaMnAs semiconductor has been detected experimentally.[14] Such an AB oscillation in a ferromagnetic ring has been studied theoretically, suggesting that a dynamical phase can exist under a special condition that a ferromagnetic ring possesses perpendicular anisotropy.[15,16]

The purpose of this paper is to further explore the effect of ferromagnets upon the electron quantum phase by using a metallic nanoring, consisting of a trilayered FeNi/Cu/FeNi structure known as a current-in-plane (CIP) giant magnetoresistive (GMR) spin valve. Electron transport in this system is confined mainly in the Cu layer, and is affected by an inhomogeneous magnetic field as well as spin-dependent interaction at the FeNi/Cu interfaces, both of which originate from the magnetization of the FeNi layers. Electrons are, therefore, expected to sense both geometrical and dynamical phases during the transport. In the CIP spin valve, magnetization configurations of the two ferromagnetic layers can be controlled to be either parallel or antiparallel, and accordingly the contribution of the geometrical phase can be changed and detected as a modulation of the dynamical phase (AB oscillation). Our results demonstrate that both the AB amplitude and frequency modulate with respect to the magnetization configurations, confirming that the phase modulation is realized in such a metallic nanoring and is induced by the existence of the ferromagnets.

The samples were in the form of an electron interferometer, consisting of the CIP-GMR spin-valve structure with wires (arms) attached to the ring edges [see the inset of Fig. 1(a)]. These structures were fabricated from an $Fe_{19}Ni_{81}$ (20 nm)/Cu (10 nm)/$Fe_{19}Ni_{81}$ (5 nm) trilayer by using a combination of electron beam lithography and lift-off techniques.[17] The sample was then mounted in a ^{3}He-^{4}He dilution refrigerator in order to perform quantum transport measurement with using a conventional four-probe method. An external magnetic field was applied with a tilting angle θ from the arm axis to control the magnetization configurations and to retain a magnetic flux penetrating inside the nanoring as schematically shown in Fig. 1(b). Here, the angle θ was fixed to be 60 deg and the magnitude of the field B_{ext} was changed at the rate of 0.1 mT/sec.

Figure 1(a) contains magnetoresistance data for both the magnetizing and demagnetizing processes at 250 mK. During the magnetizing process, the magnetoresistance exhibits discrete changes in the range $0.2 < B_{ext} < 0.6$ T, signaling considerable magnetoresistance (GMR $\sim$1.5%). When $B_{ext} > 0.6$ T, on the other hand, the magnetoresistance gradually decreases and almost saturates at $B_{ext} \sim 2$ T [anisotropic magnetoresistance (AMR) $\sim$1.2%]. Since these magnetic behaviors are found to be the same as those for the unpatterned trilayer, the magnetization configurations in the interferometer are determined by GMR and AMR hereafter. With increasing the external field from negative saturation, the parallel magnetization configuration along the ring transforms into the antiparallel configuration due to the magnetization reversal in the thinner layer,[17] and finally changes back to the

 ©2008 The American Physical Society

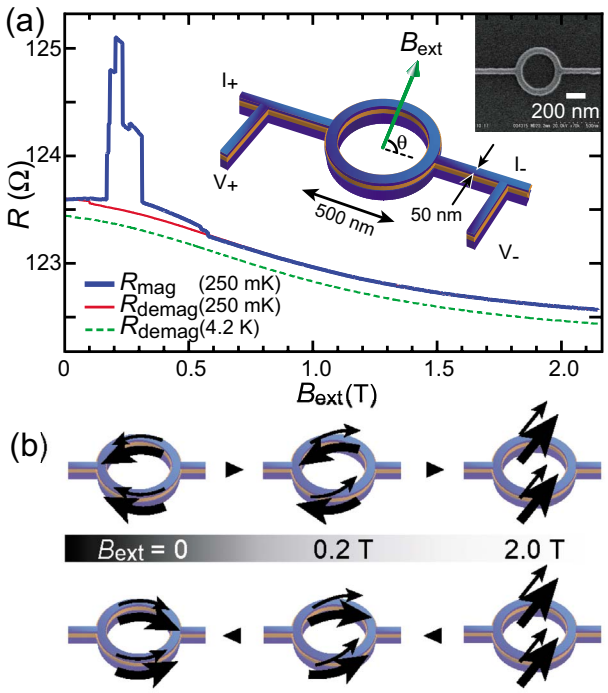

FIG. 1. (Color online) (a) Magnetic-field dependence of the resistance, exhibiting both discrete changes originating from GMR (1.5%) and gradual decreases with increasing the B_{ext} due to AMR (1.2%). The inset shows both a SEM image and a schematic illustration of the trilayered nanoring structure. The outer diameter D_o and inner diameter D_i of the ring are measured to be 500 and 400 nm, respectively, within $\pm 5\%$ accuracy. (b) Magnetization configurations under the representative field application for both the magnetizing (upper figures) and demagnetizing processes (lower figures).

parallel configuration but along the external field [see the upper figures in Fig. 1(b)]. On the other hand, the magnetoresistance in the demagnetizing process only exhibits AMR, meaning that the magnetization gradually rotates into the film plane and is curved along the circumference [the lower figures in Fig. 1(b)]. Such an AMR behavior is similarly observed in the magnetoresistance at 4.2 K [Fig. 1(a)].

In our experiment, the AB oscillation is evaluated by calculating the resistance difference $\Delta R = R(250\ \mathrm{mK}) - R(4.2\ \mathrm{K})$, which enables us to subtract the contribution of AMR and system noise as follows:

$$R_{mag}(250\ \mathrm{mK}) = R_{AB} + R_{GMR} + R_{AMR} + R_N,$$

$$R_{demag}(250\ \mathrm{mK}) = R_{AB} + R_{AMR} + R_N,$$

$$R_{demag}(4.2\ \mathrm{K}) = R_{AMR} + R_N,$$

where R_{AB}, R_{GMR}, R_{AMR}, and R_N represent the resistance contributions of the AB effect, GMR, AMR, and system noise, respectively. The ΔR is displayed in the inset of Fig. 2, where a periodic oscillation is clearly found to be superimposed on a slowly fluctuating background for both magnetizing and demagnetizing process.[18] Fourier power spectrum for corresponding ΔR exhibits a reproducible peak at 22 T^{-1},

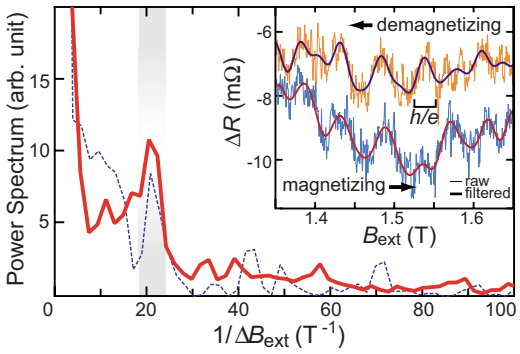

FIG. 2. (Color online) Fourier power spectra calculated from $\Delta R = R(250\ \mathrm{mK}) - R(4.2\ \mathrm{K})$ in the range $1.2 < B_{ext} < 2.0$ T, showing a large peak at 22 T^{-1}. The solid and broken lines correspond to the spectrum for ΔR_{demag} and ΔR_{mag}, respectively. The oscillations in the ΔR and Fourier-filtered curves are also shown in the inset. Here, the background offset is subtracted by adjusting the ΔR for $B_{ext} = 0$ to be zero.

and the peak frequency is found to be slightly smaller than an expected AB frequency range $24 < 1/\Delta B_{ext} < 45\ T^{-1}$, based on conventional estimation.[2,5,13] The feature is confirmed in the other three magnetoresistance traces, showing the reproducible 22 T^{-1} peak. It should be pointed out that the conventional estimation neglects the existence of the magnetization M, which generates an internal field opposite to the external magnetic field and leads to complex magnetic-field dependence of the AB oscillation. This small but clear shift of the frequency from the estimation is, therefore, a signature of the modulation of the electron quantum phase, which is induced by the ferromagnet magnetization.

To further investigate the modulation of the electron quantum phase, a wavelet analysis is carried out for $\Delta R = R_{demag}(250\ \mathrm{mK}) - R_{demag}(4.2\ \mathrm{K})$ and the wavelet transformation $w(1/\Delta B_{ext}, B_{ext})$ of the ΔR is calculated using the following formula:

$$w = \int_{-\infty}^{\infty} dx \frac{1}{\sqrt{|\Delta B_{ext}|}} \psi\left(\frac{x - B_{ext}}{\Delta B_{ext}}\right) \Delta R(x), \qquad (1)$$

where ψ represents the wavelet mother function (Gabor function).[19] $W = |w|^2$ corresponds to the power of local oscillation around B_{ext} with the frequency $\sim 1/\Delta B_{ext}$.

Figure 3(a) shows a contour plot of the power W for the trilayered nanoring, demonstrating both destructive and constructive phase modulations. Under a strong field $B_{ext} > 1.2$ T, the W exhibits a considerable magnitude at the frequency $1/\Delta B_{ext} \sim 22\ T^{-1}$ as observed in Fig. 2. With decreasing the B_{ext} from 1.2 T, the brighter area gradually changes its position. The frequencies of brighter area are observed at 0.6, 0.4, and 0.15 T for 30, 40, and 50 T^{-1}, respectively. The frequency modulation accompanies a reduction of the oscillation amplitude down to $B_{ext} \sim 0.4$ T. The oscillation amplitude in $1.2 < B_{ext} < 2$ T is estimated to be $1.2 \times 10^{-3} e^2/h$ in the conductance unit, while those at both 0.6 T and 0.4 T to be $0.6 \times 10^{-3} e^2/h$. Surprisingly, in the weak field range $B_{ext} < 0.15$ T, the amplitude is enhanced to be $1.0 \times 10^{-3} e^2/h$ and another oscillation frequency is

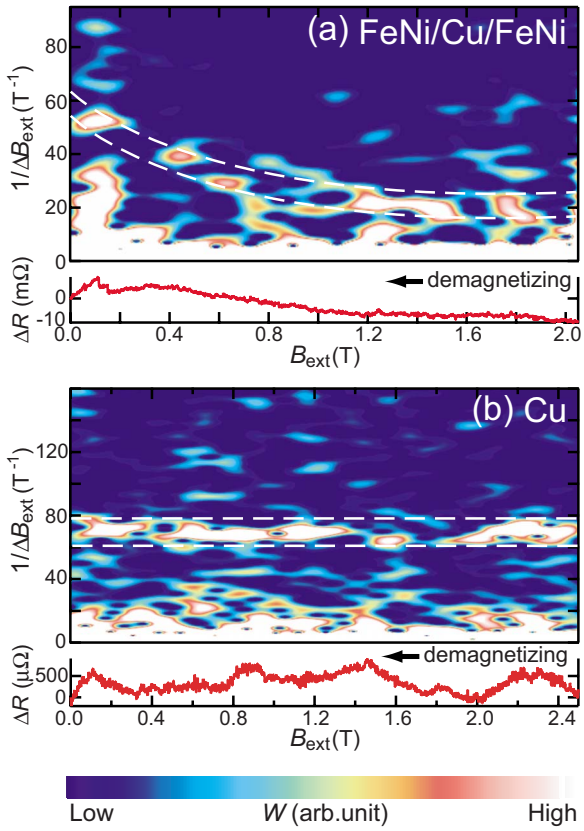

FIG. 3. (Color online) Contour plots of the $W(1/\Delta B_{\mathrm{ext}}, B_{\mathrm{ext}})$ for the cases of (a) the trilayered nanoring and (b) the single-layer Cu nanoring. The brighter area represents the larger magnitude of the W, while the darker area denotes the smaller W. The corresponding ΔR is also shown at the bottom of each figure, which shows the local oscillation characterized by the W. The boundary of the AB oscillation is drawn as dashed lines in each figure. The brighter area observed below 10 T^{-1} is due to the background fluctuation.

emerged around 30 T^{-1}, indicating a different contribution appears in the oscillation. On the other hand, the W for a single-layer Cu nanoring (D_{o}=560 nm, t=40 nm, T =150 mK) exhibits no such features as shown in Fig. 3(b). The AB frequency in the nonmagnetic Cu nanoring is constant ($\sim$70 T^{-1}) in the entire range of the applied field, showing good agreement with the expected AB frequency $62<(1/\Delta B_{\mathrm{ext}})<77$ T^{-1}. The AB amplitude conserves the magnitude of $1.6\times10^{-2}e^2/h$. These results clearly indicate that the quantum oscillations are modulated by the introduction of the magnetization with an out-of-plane component.

Magnetization configuration modulates the AB frequency, indicating that electrons acquire an additional phase. In the CIP-GMR spin-valve structure, the primary carriers are considered to be the s-like majority and minority spins originated from the Cu layer, which sense an inhomogeneous field or encounter spin-dependent scattering at the FeNi/Cu interfaces. These are possible sources to induce the geometrical phase to the electron spins in the nanoring. On the contrary, the conventional dynamical phase cannot explain the frequency modulation, since the applied magnetic field periodicity is different from $(h/e)/S$ where S is the surface of the ring under the presence of ferromagnetic layers. In addition, the dynamical phase does not include a reduction of the amplitude in the frequency modulation.

To discuss the origin of the phase modulation, the reduction of the AB amplitude is analyzed as follows. In the demagnetizing process, the majority spins are less affected from spin-dependent scattering at the interfaces. Since the magnetizations of the ferromagnetic layers are aligned parallel [Fig. 1(b)], the majority spins have similar band in the entire sample, resulting in a flat potential. However, as demonstrated in the magnetoresistance and the magnetization configurations (Fig. 1), even majority spins are subjected to AMR at FeNi/Cu interfaces, which is originated from the spin-orbit scattering in magnetic metals.[20] Theoretically, the spin-orbit scattering is known to modify the flux dependence of the dynamical phase.[21] Recently, a similar effect has been observed in a semiconductor system with using an intrinsic spin-orbit scattering under a large magnetic field application.[22] The spin-orbit scattering at the interface is, therefore, the origin of the phase modulation. This is consistent with the fact that the magnitude of oscillation amplitude becomes larger in $1.2<B_{\mathrm{ext}}<2$ T, since the magnetizations align parallel and the contribution of AMR (i.e., spin-orbit scattering) becomes smaller. Although it is not clear at present whether the phase discussed here is identical to the geometrical phase, the observed phase modulation strongly suggests the role of the magnetizations onto the quantum phase effect.

Finally, we discuss the enhancement of the oscillation amplitude in the weak field, which provides striking information regarding the phase modulation. In a strict sense, the quantum transport in a metallic system should be argued in terms of quantum corrections with using a cooperon and a diffusion propagator.[23] The cooperon represents an interference effect and is immediately demolished under the presence of a magnetic flux, whereas the diffuson represents the diffusive motion of the electrons and survives under a magnetic field. The former typically induces the AAS $(h/2e)$ oscillation, while the latter induces the AB (h/e) oscillation,[16] which means that the larger amplitudes in the weak field corre-

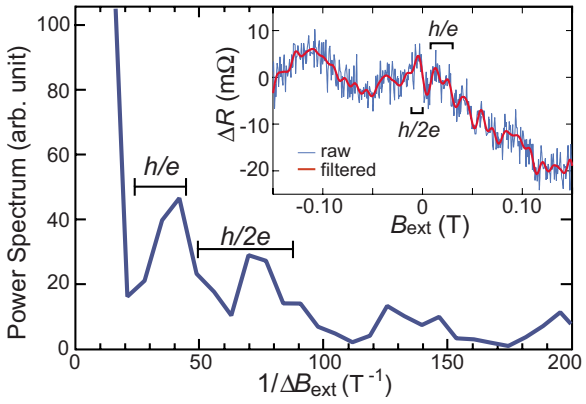

FIG. 4. (Color online) Fourier power spectrum deduced from $\Delta R=R_{\mathrm{demag}}(120\ \mathrm{mK})-R_{\mathrm{demag}}(4.2\ \mathrm{K})$ in the weak field range $|B_{\mathrm{ext}}|<0.15$ T. The ΔR and the Fourier-filtered curve, in which the background are subtracted, are also shown in the inset. The asymmetry of the ΔR originates from the hysteresis of the magnetization curve.

sponds to the contribution of the cooperon. The contribution of the cooperon is confirmed by the magnetoresistance measurement performed at lower temperature (120 mK). Figure 4 shows the Fourier power spectrum deduced from the magnetoresistance in the range $|B_{\mathrm{ext}}| < 0.15$ T with revealing two distinct peaks at 42 T^{-1} and 70 T^{-1}. As shown in the inset of Fig. 4, the $h/2e$ oscillation is visible in the weaker field range $|B_{\mathrm{ext}}| < 0.04$ T, however, it immediately becomes indistinguishable under the stronger field. In general, the interference effect given by the cooperon is considered to be dominant within the dephasing length $L_B \equiv \sqrt{12}(\hbar/eaB)$, where a is the width of the ring.[16] The dephasing length in our sample is roughly estimated to be 1.2 μm by using the film-normal component of the applied magnetic field $B_{\mathrm{ext}\perp} \sim 0.04 \sin(60°)$ T, since the contribution of magnetic domains is negligible in this small range of magnetic field. While the circumference of the ring is estimated to be in the range $1.2 \leq L \leq 1.6$ μm, which is comparable to the L_B. Thus, the cooperon can survive under our experimental condition.

In conclusion, low-temperature magnetoresistance in a trilayered nanoring unambiguously shows the influence of ferromagnets upon the Aharonov-Bohm (AB) oscillation. The wavelet analysis reveals the detailed field-dependence of the AB oscillation, presenting clear distinction from that of a single-layered nonmagnetic nanoring. The frequency increases and the amplitude decreases with decreasing an external field, which is contrary to the conventional flux dependence of the quantum dynamical phase. Fourier analysis further demonstrates that different oscillation components are superimposed to the magnetoresistance in a weak field, which proves the existence of the quantum interference. These results suggest that the trilayered nanoring system is ideal for systematic investigation of the influence of ferromagnets upon electron quantum coherence.

One of the authors (K.S.) was supported by the Japan Society for the Promotion of Science (JSPS).

*kojisekiguchi@riken.jp

[1] Y. Imry, *Introduction to Mesoscopic Physics* (Oxford University Press, Oxford, 1977).
[2] R. A. Webb, S. Washburn, C. P. Umbach, and R. B. Laibowitz, Phys. Rev. Lett. **54**, 2696 (1985).
[3] S. Washburn, C. P. Umbach, R. B. Laibowitz, and R. A. Webb, Phys. Rev. B **32**, 4789 (1985).
[4] C. P. Umbach, C. Van Haesendonck, R. B. Laibowitz, S. Washburn, and R. A. Webb, Phys. Rev. Lett. **56**, 386 (1986).
[5] R. Haussler, E. Scheer, H. B. Weber, and H. v. Lohneysen, Phys. Rev. B **64**, 085404 (2001).
[6] M. V. Berry, Proc. R. Soc. London, Ser. A **392**, 45 (1984).
[7] J. J. Sakurai, *Modern Quantum Mechanics* (Addison-Wesley, Redwood City, CA, 1994).
[8] A. Shapere and F. Wilczek, *Geometric Phases in Physics* (World Scientific, Singapore, 1989).
[9] D. Loss, P. Goldbart, and A. V. Balatsky, Phys. Rev. Lett. **65**, 1655 (1990).
[10] L. P. Levy, G. Dolan, J. Dunsmuir, and H. Bouchiat, Phys. Rev. Lett. **64**, 2074 (1990).
[11] J. B. Yau, E. P. DePoortere, and M. Shayegan, Phys. Rev. Lett. **88**, 146801 (2002).
[12] G. Tatara and H. Kohno, Phys. Rev. B **67**, 113316 (2003).
[13] S. Kasai, T. Niiyama, E. Saitoh, and H. Miyajima, Appl. Phys. Lett. **81**, 316 (2002).
[14] L. Vila, R. Giraud, L. Thevenard, A. Lemaitre, F. Pierre, J. Dufouleur, D. Mailly, B. Barbara, and G. Faini, Phys. Rev. Lett. **98**, 027204 (2007).
[15] G. Tatara and B. Barbara, Phys. Rev. B **64**, 172408 (2001).
[16] G. Tatara, H. Kohno, E. Bonet, and B. Barbara, Phys. Rev. B **69**, 054420 (2004).
[17] K. Sekiguchi, A. Yamaguchi, and H. Miyajima, J. Magn. Soc. Jpn. **31**, 77 (2006).
[18] The oscillation component of the magnetizing processes is identical to that of the demagnetizing process, except for the field range $0.2 < B_{\mathrm{ext}} < 0.5$ T, where no oscillation behavior is obtained, indicating the spin-flip scattering with the antiparallel configuration demolishes the electron coherence. As shown in Fig. 2, the background resistance between the magnetizing and demagnetizing processes is very different, suggesting the presence of the magnetic hysteresis. However, the resistance oscillation becomes identical once the magnetization is almost saturated, indicating the validity of our discussion on the quantum spin transport.
[19] C. K. Chui, *An Introduction to Wavelets* (Academic Press, New York, 1992).
[20] T. R. McGuire and R. I. Potter, IEEE Trans. Magn. **11**, 1018 (1975).
[21] Y. Meir, Y. Gefen, and O. Entin-Wohlman, Phys. Rev. Lett. **63**, 798 (1989).
[22] B. Grbić, R. Leturcq, T. Ihn, K. Ensslin, D. Reuter, and Andreas D. Wieck, Phys. Rev. Lett. **99**, 176803 (2007).
[23] B. L. Altshuler and A. G. Aronov, in *Electron-Electron Interactions in Disordered Systems*, edited by A. L. Efros and M. Pollak (Elsevier, New York, 1985).